

# Spin entanglement induced by spin-orbit interactions in coupled quantum dots

Nan Zhao,<sup>1</sup> L. Zhong,<sup>2</sup> Jia-Lin Zhu,<sup>1</sup> and C. P. Sun<sup>2</sup>

<sup>1</sup>*Department of Physics, Tsinghua University, Beijing 100084, China*

<sup>2</sup>*Institute of Theoretical Physics, Chinese Academy of Sciences, Beijing, 100080, China*

We theoretically explore the possibility of creating spin quantum entanglement in a system of two electrons confined respectively in two vertically coupled quantum dots in the presence of Rashba type spin-orbit coupling. We find that the system can be described by a generalized Jaynes - Cummings model of two modes bosons interacting with two spins. The lower excitation states of this model are calculated to reveal the underlying physics of the far infrared absorption spectra. The analytic perturbation approach shows that an effective transverse coupling of spins can be obtained by eliminating the orbital degrees of freedom in the large detuning limit. Here, the orbital degrees of freedom of the two electrons, which are described by two modes of bosons, serve as a quantized data bus to exchange the quantum information between two electrons. Then a nontrivial two-qubit logic gate is realized and spin entanglement between the two electrons is created by virtue of spin-orbit coupling.

PACS numbers: 73.63.Kv, 03.65.-w, 03.67.Mn, 71.70.Ej

## I. INTRODUCTION

Control and manipulation of the spin degree of freedom become one of the most important topics both in spintronics[1] and in quantum information processing [2]. The spin-orbit interactions (SOI) in semiconductor heterostructures provides the ways to couple spin with spatial degree of freedom, and consequently has attracted more and more attention in recent years. The spin properties of a few electrons confined in semiconductor nanostructures, such as quantum dots[3, 4, 5, 6, 7, 8], coupled quantum dots[9], quantum rings[10] and quantum wires[11], have been studied. The results show that the carrier spin properties are strongly affected in the presence of the SOI, and novel features emerge in these nonstructures compared with the traditional ones without SOI.

On the other hand, spin confined in quantum dot is a natural choice for the physical realization of qubit. This kind of system is considered as an important candidate for solid state based quantum computing. Among various approaches to implement quantum information processing using quantum dot systems, the optical method, including the classical laser field[12] and the quantized cavity modes [13], has been proposed to create entanglement and to realize the single and double qubit logic gate. In Ref. [15], a scheme with quantum dots embedded in an optical cavity was designed, so that the cavity mode can serve as a data bus and induce a spin-spin interaction. This kind of cavity-mediated two-qubit gate is studied in details for several other solid state systems very recently[16].

Now we notice that the SOI phenomena in nanostructures were investigated with the help of the quantum optics method. Taking advantage of the tunability of the SOI strength, an experiment to observe coherent oscillations in a single quantum dot was proposed in ref. [3]. In this proposal, the orbital degrees of freedom are modeled by two boson modes. Under the rotating wave approx-

imation (RWA), the SOI of the electron confined in the single quantum dot, is reduced to a Jaynes- Cummings (JC) model, which is very typical model in quantum optics. This analogy between the SOI in a quantum dot and the JC model in cavity QED suggests us that it is possible to make use of the orbital degree of freedom, instead of the real optical cavity modes, to serve as a quantized data bus and then to induce a spin entanglement[14].

In this paper, we propose and study a model of two electrons confined in two quantum dots respectively with Rashba type SOI, and explore the possibility of realizing a two-qubit logic gate or creating spin entanglement with this system. For simplicity, we consider two vertically coupled quantum dots (CQDs) with two dimensional parabolic confinements. In the case with strong confinement and large interdot separation, the Coulomb interaction between the two electrons is approximately expanded in a quadratic form, and then the orbital part of the two electron system can be reduced to four-mode bosons. Under the RWA, only two of the four modes are coupled with the spin degrees of freedom. Then it is proved that the total system with SOI can be effectively described by a generalized JC model with the coupling between two bosons and two spins. By diagonalizing the Hamiltonian directly in the lower excitation subspace, the eigenvalues and the corresponding eigenfunction are obtained exactly. The far infrared (FIR) absorption spectra are calculated according to these analytical solutions, which help us to understand the underlying physics of the spectra. To get an effective Hamiltonian of spin-spin interaction, we perform the Fröhlich transformation in the large detuning limit. This effective Hamiltonian can dynamically drive a two-qubit logic gate operation. By using the conventional material parameters, our numerical estimation shows that the effective spin interaction induced by SOI is strong enough, compared to the spin decoherence in low dimensional semiconductor structures. It is feasible experimentally to implement a two-qubit logic gate and thus produce quantum entanglement.

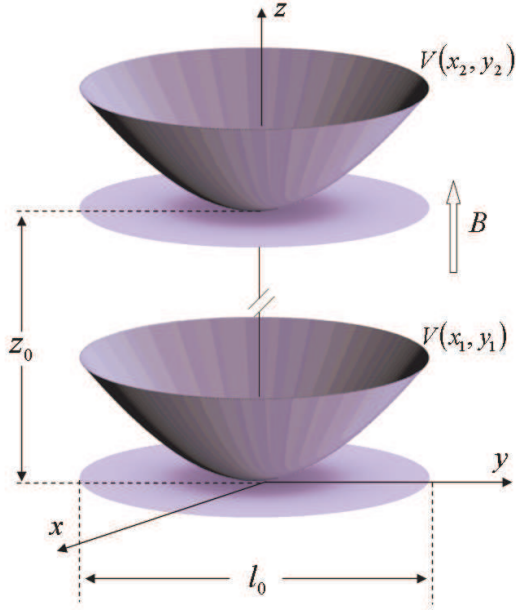


FIG. 1: Schematic illustration of the vertically stacked quantum dots. Each quantum dot confined an electron. We assume that the interdot separation  $z_0$  is larger than the characteristic length of quantum dot confinement  $l_0$ .

The paper is organized as follows. In Section II, the two modes JC model is derived from the conventional Hamiltonian of two electrons confined in two quantum dots. Analytical solution of lower excitation states and FIR spectra are presented in Section III. In Section IV, we show that the perturbation treatment gives the effective transverse spin-spin interaction in the large detuning limit, and demonstrate that a two-qubit logic gate and quantum entanglement can be achieved in this kind system with SOI.

## II. TWO MODES JC MODEL FOR VERTICALLY CQDS WITH SOI

We consider two vertically CQDs with an interdot separation  $z_0$ , see Fig.1. Each quantum dot is described by a two dimensional parabolic confinement potential  $V(r_i) = m_0\omega_0^2 r_i^2/2$  with the basic frequency  $\omega_0$ . Including the Rashba type SOI

$$H_{SO}^{(i)} = \frac{\alpha}{\hbar} [\sigma_i \times \mathbf{\Pi}_i]_z, \quad (1)$$

the Zeeman term

$$H_Z^{(i)} = \frac{1}{2} g \mu_B \mathbf{B} \cdot \sigma_i, \quad (2)$$

and the Coulomb interaction

$$V_{coul}(|\mathbf{r}_1 - \mathbf{r}_2|) = \frac{e^2}{4\pi\epsilon\epsilon_0 |\mathbf{r}_1 - \mathbf{r}_2|}, \quad (3)$$

the total Hamiltonian reads:

$$H = \sum_{i=1,2} \left( \frac{\mathbf{\Pi}_i^2}{2m_0} + V(r_i) + H_{SO}^{(i)} + H_Z^{(i)} \right) + V_{coul}. \quad (4)$$

Here,  $-e$ ,  $\mu_B$  and  $\epsilon_0$  are the electron charge, Bohr magneton and dielectric constant in vacuum,  $m_0$ ,  $g$  and  $\epsilon$  are the material related parameters of effective mass, Landre g-factor and the relative dielectric constant, respectively.  $\mathbf{\Pi}_i = \mathbf{p}_i + e\mathbf{A}(\mathbf{r}_i)$  is the canonical momentum and  $\mathbf{A}(\mathbf{r}_i) = B(-y_i/2, x_i/2, 0)$  is the vector potential for magnetic field  $\mathbf{B} = B\hat{\mathbf{z}}$ .

In order to simplify the Coulomb interaction, we consider a special case in which the interdot separation  $z_0$  is much larger than the lateral confinement characteristic length  $l_0 = \sqrt{\hbar/m_0\omega_0}$ , i.e.  $(l_0/z_0)^2 \ll 1$ . Then we expand the Coulomb interaction as a power series of the relative coordinate  $r = |\mathbf{r}_1 - \mathbf{r}_2|$  up to the second order[17][18]:

$$V_{coul}(r) \simeq V_0 - \frac{1}{2} m_0 \omega_1^2 r^2. \quad (5)$$

Here, we have defined  $V_0 = e^2/(4\pi\epsilon\epsilon_0 z_0)$ , and  $\hbar\omega_1 = \sqrt{\hbar^2 V_0/mz_0^2}$ . We also assume that electrons are strictly confined in each quantum dots planes, and then neglect the overlap of their wavefunctions.

In the center of mass (CM) reference of frame defined by  $\mathbf{R} = (\mathbf{r}_1 + \mathbf{r}_2)/2$  and  $\mathbf{r} = \mathbf{r}_1 - \mathbf{r}_2$ , we have the C.M. and relative momentums, and the corresponding angular momentums  $\mathbf{P} = \mathbf{p}_1 + \mathbf{p}_2$ ,  $\mathbf{p} = \frac{1}{2}(\mathbf{p}_1 - \mathbf{p}_2)$ ,  $\mathbf{L} = \mathbf{R} \times \mathbf{P}$ , and  $\mathbf{l} = \mathbf{r} \times \mathbf{p}$ , where  $M = 2m_0$ ,  $m = m_0/2$ ,  $\mathbf{r}$  is the relative coordinate and  $\mathbf{R}$  the CM coordinate. The orbital part of the Hamiltonian is expressed in a quadrature form of these coordinates:

$$\begin{aligned} H_{orbit} &= \sum_{i=1,2} \left( \frac{\mathbf{\Pi}_i^2}{2m_0} + V(r_i) \right) + V_{coul} \\ &= \frac{P^2}{2M} + \frac{1}{2} M \Omega^2 R^2 + \frac{1}{2} \omega_c L_z \\ &\quad + \frac{p^2}{2m} + \frac{1}{2} m \omega^2 r^2 + \frac{1}{2} \omega_c l_z \end{aligned} \quad (6)$$

Here, the cyclone frequency is  $\omega_c = eB/m_0$ , and frequency of CM and relative motion  $\Omega = \sqrt{\omega_0^2 + \omega_c^2/4}$  and  $\omega = \sqrt{\Omega^2 - 2\omega_1^2}$ , respectively. Note that the effect of the Coulomb repulsion is reducing the relative motion to a lower frequency compared to the CM motion. In our model the requirement  $(l_0/z_0)^2 \ll 1$  ensures that the  $\omega > 0$  is satisfied even when  $B = 0$ .

We define the boson operators  $a_x, a_x^\dagger, a_X, a_X^\dagger$  of  $x$  com-

Quantity	Value	Unit	Quantity	Value	Unit
$m_0$	0.042	-	$\omega_0$	20	meV
$\varepsilon$	14.6	-	$l_0$	9.5	nm
$g$	-14	-	$z_0$	20	nm
$\alpha$	10	meV·nm			

TABLE I: Parameters used in the calculations

ponents by

$$\begin{aligned}
X &= \sqrt{\frac{\hbar}{2M\Omega}} (a_X^+ + a_X), \\
x &= \sqrt{\frac{\hbar}{2m\omega}} (a_x^+ + a_x), \\
P_X &= i\sqrt{\frac{\hbar M\Omega}{2}} (a_X^+ - a_X), \\
p_x &= i\sqrt{\frac{\hbar m\omega}{2}} (a_x^+ - a_x)
\end{aligned} \tag{7}$$

and the boson operators  $a_y, a_y^+, a_Y, a_Y^+$  of  $y$  components are defined in the same way. Let

$$\begin{aligned}
A &= (a_X + ia_Y) / \sqrt{2}, \\
a &= (a_x + ia_y) / \sqrt{2}, \\
B &= (a_X - ia_Y) / \sqrt{2}, \\
b &= (a_x - ia_y) / \sqrt{2}.
\end{aligned} \tag{8}$$

Then we rewrite orbit Hamiltonian (6)

$$\begin{aligned}
H_{\text{orbit}} &= \hbar\omega_A (A^+ A + 1/2) + \hbar\omega_B (B^+ B + 1/2) \\
&+ \hbar\omega_a (a^+ a + 1/2) + \hbar\omega_b (b^+ b + 1/2)
\end{aligned} \tag{9}$$

in terms of four mode bosons  $A, a, B,$  and  $b$ , with their frequencies respectively

$$\omega_A = \Omega - \frac{1}{2}\omega_c, \omega_B = \Omega + \frac{1}{2}\omega_c, \tag{10}$$

$$\omega_a = \omega - \frac{1}{2}\omega_c, \omega_b = \omega + \frac{1}{2}\omega_c \tag{11}$$

These four frequencies, together with the Zeeman energy  $\hbar\omega_z = |g|\mu_B B$  are drawn in Fig.2 with respect to the magnetic field  $B$ . Note that the Zeeman energy  $\hbar\omega_z$  and the boson frequencies  $\omega_A$  and  $\omega_a$  reach the resonant regime at  $B \simeq 11T$  with the parameters listed in Table I. We also draw the lower energy spectra of the orbit Hamiltonian (6) in Fig.2(b). We will focus on how these states are affected in the presence of SOI in the following sections.

In terms of the four boson operators defined by Eqs. (7) and (8), the SOI Hamiltonian  $H_{SO}$ , after some straightforward algebra, can be rewritten as:

$$\begin{aligned}
H_{SO}^{RWA} &= g_A \cdot A (\sigma_{1+} + \sigma_{2+}) \\
&+ g_a \cdot a (\sigma_{1+} - \sigma_{2+}) + h.c.
\end{aligned} \tag{12}$$

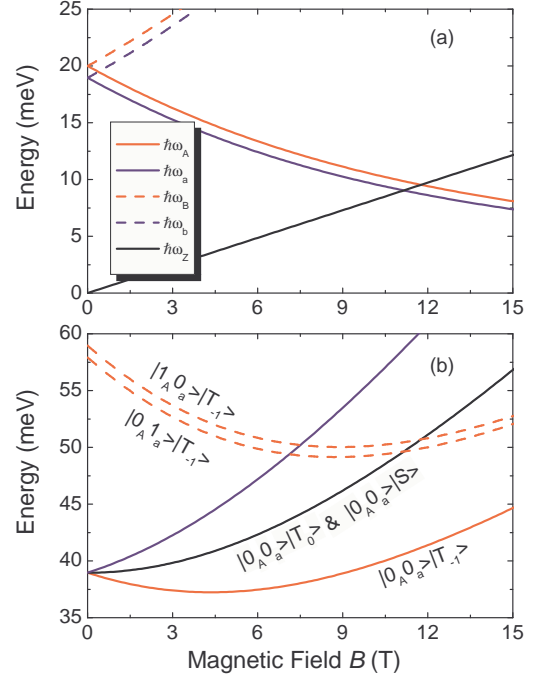


FIG. 2: (a) Energy dispersions with respect to the magnetic field  $B$  of the four modes of the boson frequencies  $\omega_A$  (red solid line),  $\omega_a$  (blue solid line),  $\omega_B$  (red dashed line), and  $\omega_b$  (blue dashed line), and the Zeeman energy  $\omega_z$  (black line). (b) Energy spectrum of  $H_0$ . Different lines correspond to different spin and orbit states, which are indicated explicitly in the figure. The parameters used in calculation are listed in Table I

Note that, due to the negative value of the Landre g-factor, a unitary rotation  $\sigma_z \mapsto -\sigma_z$  and  $\sigma_{\pm} \mapsto -\sigma_{\mp}$  has been performed. To obtain the interaction Hamiltonian above, we have used the RWA to neglect the counter-rotating terms like  $\sigma_+ B^+$ ,  $\sigma_+ b^+$ ,  $\sigma_- B$ , and  $\sigma_- b$ . This approximation has been verified numerically for single electron case in Ref. [3]. The coupling strengths  $g_A$  and  $g_a$  are defined as follows:

$$g_A = \alpha \sqrt{\frac{m_0 \Omega}{2\hbar}} \left(1 - \frac{\omega_c}{2\Omega}\right) \tag{13}$$

$$g_a = \alpha \sqrt{\frac{m_0 \omega}{2\hbar}} \left(1 - \frac{\omega_c}{2\omega}\right) \tag{14}$$

So far, we have obtained a generalized JC model where two-mode bosons interact with two spins. In the following sections we will further demonstrate how the orbit motion induce a spin-spin entanglement in the presence of SOI.

### III. LOWER EXCITATION STATES AND FIR SPECTRA

In this section, we calculate the eigenenergies and eigenstates of the low excitation states. Notice that the

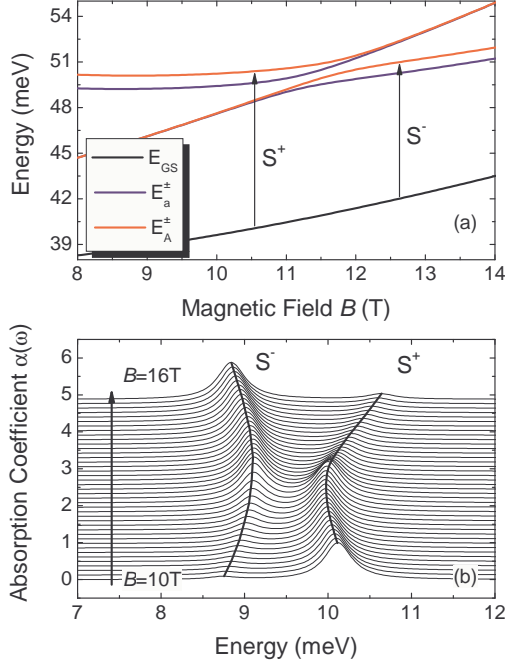


FIG. 3: (a) Exact energy spectra given by Eqs.(23) and (24). The arrows indicate the dipole allowed transition from  $|GS\rangle$  (black line) to  $|\Phi_A^\pm\rangle$  (red lines).  $|\Phi_a^\pm\rangle$  (blue lines) is dipole inactive. (b) FIR spectra for increasing magnetic field  $B$ . The anti-crossing is clearly shown. A Lorentz profile function  $\Gamma/\pi[(\omega - \omega_{fi}) - \Gamma^2]$  is used to replace the  $\delta$  function. The phenomenological broaden factor  $\Gamma = 0.2\text{meV}$ . Spectra are normalized to their maxima and offset for clarity.

total excitation number operator

$$\hat{N} = a^\dagger a + A^\dagger A + \frac{1}{2}(\sigma_{1z} + \sigma_{2z}) \quad (15)$$

commutes with  $H = H_{\text{orbit}} + H_Z^{(1)} + H_Z^{(2)} + H_{SO}^{RWA}$ . For a given integer  $N$ , which is the eigenvalue of  $\hat{N}$ , the dimension of the invariant subspace  $V^{(N)}$  is  $4N + 4$  for  $N \geq 0$ .

The lowest subspace  $V^{(-1)}$ , corresponding to  $N = -1$ , is of one dimension. The the ground state can be directly written as  $|GS\rangle = |0_A, 0_a, 0_B, 0_b, \downarrow, \downarrow\rangle$ , which means the excitation numbers of boson modes

$$A^\dagger A = a^\dagger a = B^\dagger B = b^\dagger b = 0 \quad (16)$$

and both spins are in the down state. The corresponding eigenenergy is

$$E_{GS} = \frac{\hbar}{2}(\omega_A + \omega_B + \omega_a + \omega_b - 2\omega_z). \quad (17)$$

The second lowest subspace  $V^{(0)}$ , which is of four dimension. The Hamiltonian can be exactly diagonalized in

this subspace. We define

$$\begin{aligned} |S\rangle &= \frac{1}{\sqrt{2}}(|0_A, 0_a, \uparrow, \downarrow\rangle - |0_A, 0_a, \downarrow, \uparrow\rangle), \\ |T_0\rangle &= \frac{1}{\sqrt{2}}(|0_A, 0_a, \uparrow, \downarrow\rangle + |0_A, 0_a, \downarrow, \uparrow\rangle), \\ |T_{-1}^A\rangle &= |1_A, 0_a, \downarrow, \downarrow\rangle, |T_{-1}^a\rangle = |0_A, 1_a, \downarrow, \downarrow\rangle. \end{aligned} \quad (18)$$

The eigenstates of the Hamiltonian in this subspace are

$$|\Phi_A^+\rangle = \sin \frac{\theta_A}{2} |T_{-1}^A\rangle + \cos \frac{\theta_A}{2} |T_0\rangle, \quad (19)$$

$$|\Phi_A^-\rangle = \cos \frac{\theta_A}{2} |T_{-1}^A\rangle - \sin \frac{\theta_A}{2} |T_0\rangle, \quad (20)$$

$$|\Phi_a^+\rangle = \sin \frac{\theta_a}{2} |T_{-1}^a\rangle + \cos \frac{\theta_a}{2} |S\rangle, \quad (21)$$

$$|\Phi_a^-\rangle = \cos \frac{\theta_a}{2} |T_{-1}^a\rangle - \sin \frac{\theta_a}{2} |S\rangle \quad (22)$$

and the corresponding eigenvalues are:

$$E_A^\pm = -\frac{\Delta_A}{2} \pm \sqrt{\left(\frac{\Delta_A}{2}\right)^2 + 2g_A^2}, \quad (23)$$

$$E_a^\pm = -\frac{\Delta_a}{2} \pm \sqrt{\left(\frac{\Delta_a}{2}\right)^2 + 2g_a^2}. \quad (24)$$

Here, the zero point energies of the four boson modes are omitted.  $\theta_{A,a}$  is defined as

$$\tan \theta_{A,a} = \frac{2\sqrt{2}g_{A,a}}{\Delta_{A,a}} \quad (25)$$

where  $\theta_{A,a} \in [0, \pi]$ , and  $\Delta_{A,a} = \omega_z - \omega_{A,a}$ .

With the help of these exact eigenenergies and the eigenstates obtained above, we can calculate the FIR absorption spectra analytically. To this end, we consider the time-dependent Hamiltonian of the system in an optical field is

$$\tilde{H}(t) = H + H' e^{-i\omega t} \quad (26)$$

where  $H'$  is the time dependent term induced by the classical optical field [6]

$$H' \propto - \sum_{i=1,2} \left[ \frac{ea}{m} \epsilon \cdot (\mathbf{p}_i + e\mathbf{A}_i) + \frac{\alpha ea}{\hbar} (\sigma_i \times \epsilon)_z \right] \quad (27)$$

where  $a$  is the radiation field amplitude, and  $\epsilon = (\hat{x} - i\hat{y})/\sqrt{2}$  is the polarization vectors for circular polarized light.

The absorption coefficient is calculated according to the Fermi golden rule[19][20]:

$$\alpha(\omega) \propto \omega \sum_f |\langle f | H' | i \rangle|^2 \delta(\omega - \omega_{fi}), \quad (28)$$

Here,  $\hbar\omega_{fi} = E_f - E_i$ ,  $|i\rangle = |GS\rangle$  is the ground state, and  $|f\rangle$  stands for the excited states. We will focus on

the four lowest excited states  $|\Phi_A^\pm\rangle$  and  $|\Phi_a^\pm\rangle$ . According to Eqs. (7) and (8), the perturbation  $H'$  is obtained as

$$H' = \hbar\Omega\sqrt{\frac{\omega_0}{\Omega}}\left(1 - \frac{\omega_c}{\Omega}\right)A^+ + \alpha\sqrt{\frac{2m_0\omega_0}{\hbar}}(\sigma_{1+} + \sigma_{2+}) \quad (29)$$

Note that we have omitted the terms related to the  $B$  modes, which is not involved in the initial and final states we are considering and thus does not contribute to the absorption coefficient. Our analytical results give the FIR spectra of obvious physical meanings. From Eq.(29) above, we find that the first term is spin independent, and it provides an CM angular excitation. This CM angular excitation, which is the consequence of Kohn theorem[21], exists even in the absence of SOI. The second term, which is spin dependent, is due to the presence of SOI. This term contributes an excitation of the two spins *symmetrically*, i.e.  $|\downarrow\downarrow\rangle \mapsto |\uparrow\downarrow\rangle + |\downarrow\uparrow\rangle$ . Thus,  $H'$  only couples the ground state  $|GS\rangle$  with the CM excitation states  $|\Phi_A^\pm\rangle$ , and  $|\Phi_a^\pm\rangle$  are inactive in this case. The matrix elements of  $\langle\Phi_A^\pm|H'|GS\rangle$  are calculated, and the FIR spectra are shown in Fig.3(b).

#### IV. QUANTUM ENTANGLEMENT IN LARGE DETUNING LIMIT

Due to the linearly increasing of the dimension of the invariance subspace  $V^{(N)}$  with respect to  $N$ , it is difficult

to obtain a compact solution of the eigenvalue problem for  $N \geq 1$ . Instead of the exact solution, the approximate solution by perturbation theory will be given in this section. In the perturbation available regime, we derive an effective transverse spin-spin interaction Hamiltonian. This Hamiltonian can induce a two-qubit logic gate, and can be used to produce a controllable quantum entanglement.

We summarize the Hamiltonian obtained

$$H_0 = H_{\text{orbit}} + \frac{1}{2}\hbar\omega_z(\sigma_{1z} + \sigma_{2z}), \quad (30)$$

$$H_1 = g_A \cdot A(\sigma_{1+} + \sigma_{2+}) + g_a \cdot a(\sigma_{1+} - \sigma_{2+}) + h.c. \quad (31)$$

and then consider its reduction in the large detuning limit, i.e.  $\Delta_{A,a} \gg g_{A,a}$ . In this limit, we perform the Fröhlich transform with the operator

$$S = \left( \frac{g_A}{\Delta_A} A^+ (\sigma_{1-} + \sigma_{2-}) + \frac{g_a}{\Delta_a} a^+ (\sigma_{1-} - \sigma_{2-}) \right) - h.c. \quad (32)$$

and the effective Hamiltonian  $\exp(-S)H\exp(S)$  is calculated up to the second order as:

$$H_S \simeq H_0 + \frac{1}{2}[H_1, S]. \quad (33)$$

Here, the second term in the r.h.s can be written explicitly

$$\begin{aligned} \frac{1}{2}[H_1, S] &= \hbar\xi(\sigma_{1+}\sigma_{2-} + \sigma_{1-}\sigma_{2+}) + \frac{g_A g_a}{2} \left( \frac{1}{\Delta_A} + \frac{1}{\Delta_a} \right) (A^+ a + a^+ A) (\sigma_{1z} - \sigma_{2z}) \\ &+ \left[ \frac{g_A^2}{\Delta_A} (A^+ A + 1/2) + \frac{g_a^2}{\Delta_a} (a^+ a + 1/2) \right] (\sigma_{1z} + \sigma_{2z}) + \left( \frac{g_A^2}{\Delta_A} + \frac{g_a^2}{\Delta_a} \right) \end{aligned} \quad (34)$$

Note that the first term of Eq.(34) is the effective transverse spin-spin coupling induced by SOI. The effective coupling strength

$$\hbar\xi = g_A^2/\Delta_A - g_a^2/\Delta_a \quad (35)$$

depends on (i) the SOI strength  $\alpha$  (see Eqs.(14) and (13)), and (ii) the frequency difference between  $\omega_A$  and  $\omega_a$ , which is the consequence of the Coulomb interaction. We note that, in the subspace  $V^{(0)}$ , the second term of Eq.(34) vanishes, and the remaining terms commute with the total spin  $\sigma^2 = (\sigma_1 + \sigma_2)^2$ . Thus we can denote the eigenstates by spin singlet  $|S\rangle = (|\uparrow\downarrow\rangle - |\downarrow\uparrow\rangle)/\sqrt{2}$  and triplet  $|T_0\rangle = (|\uparrow\downarrow\rangle + |\downarrow\uparrow\rangle)/\sqrt{2}$ ,  $|T_1\rangle = |\uparrow\uparrow\rangle$ , and  $|T_{-1}\rangle = |\downarrow\downarrow\rangle$  in the large detuning limit in subspace  $V^{(0)}$ . Diagonalizing the Hamiltonian (34), we obtain the

eigenenergies

$$E_{|T_{-1}\rangle} = -\Delta_A - \frac{2g_A^2}{\Delta_A}, \quad (36)$$

$$E_{|T_{-1}^a\rangle} = -\Delta_a - \frac{2g_a^2}{\Delta_a}, \quad (37)$$

$$E_{|T_0\rangle} = \frac{2g_A^2}{\Delta_A}, \quad (38)$$

$$E_{|S\rangle} = \frac{2g_a^2}{\Delta_a} \quad (39)$$

for the different spin states corresponding to the exact solutions in Eq.(24). Here, we also omit the zero point energies.

The above energies are drawn as the function of magnetic field in Fig.4(c) in comparison with the exact solution. The exact consistency of the two solutions in the

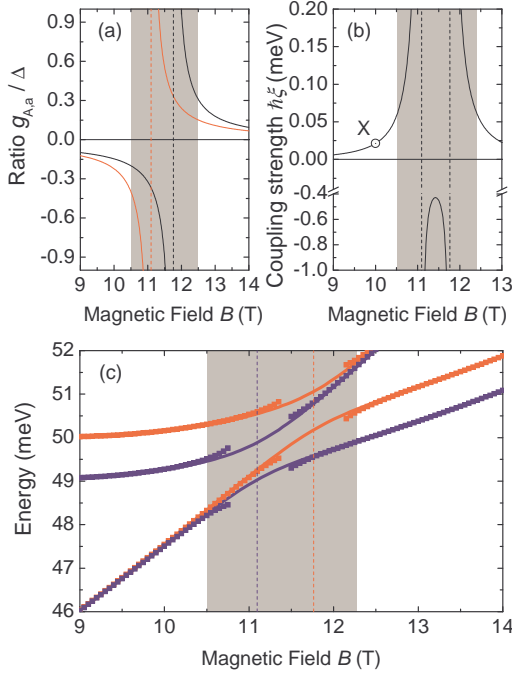


FIG. 4: (a) The ratio  $g_A/\Delta_A$  (black line) and,  $g_a/\Delta_a$  (red line). The perturbation treatment is valid when both  $g_A/\Delta_A$  and  $g_a/\Delta_a$  less than unity. (b) The effective transverse spin coupling strength induced by SOC. (c) A comparison of eigenenergies between exact (Eqs.(23) and (24), lines) and perturbative(Eqs.(36) ~ (39), scattered dots) solutions in the large detuning regime. Our perturbation treatment is valid in the unshaded region.

large detuning regime confirms the validity of our perturbation treatment. Fig.4(a) shows effective spin coupling strength induced by SOI in our model. In the perturbation valid regime, for example at  $B = 10$  T (the point denoted by X), we have the spin coupling strength  $\hbar\xi \simeq 20\mu\text{eV}$ . This value is comparable with that in the proposal of the spin-spin coupling induced by the electromagnetic field in cavity[15]. Thus, it is feasible to realize the two-qubit gate operation during the long coherence time of conduction band electrons.

The spin transverse coupling described by the first term in the r.h.s. of Eq.(34) generates an ideal  $\sqrt{i}\text{SWAP}$  gate[22][16] at a specific time  $t_0 = \pi/4\xi$ . On the other hand, it is worthy to notice that the unitary transformation  $\exp(-S)H\exp(S)$  may induce an excitation of the boson modes, and then causes gate error during the time evolution of the spin states. To explicitly show the unwanted boson modes excitation and to examine the reliability of our model, we consider the time evolution of the initial state  $|\psi(0)\rangle = |\downarrow\uparrow, 0_A, 0_a\rangle$ :

$$|\psi(t)\rangle = U(t) |\psi(0)\rangle,$$

where

$$U(t) = \exp[it(e^S H_S e^{-S})/\hbar] = e^S \exp(itH_S/\hbar) e^{-S}.$$

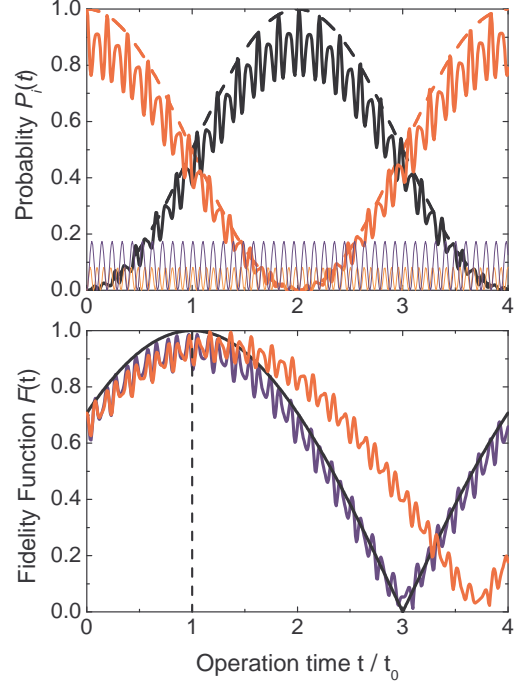


FIG. 5: (a) Probability  $P_i(t)$  as a function of  $t$ . Black, red, blue, and orange solid lines represent the probabilities of  $|\uparrow\downarrow, 0_A, 0_a\rangle$ ,  $|\downarrow\uparrow, 0_A, 0_a\rangle$ ,  $|\downarrow\downarrow, 1_A, 0_a\rangle$ , and  $|\downarrow\downarrow, 0_A, 1_a\rangle$  respectively. The dashed lines are the probabilities generated by the standard  $\sqrt{i}\text{SWAP}$  gate. (b) Gate fidelity as a function of  $t$ . The black line indicates the ideal  $\sqrt{i}\text{SWAP}$  operation. The blue and red lines represent the fidelity function generated by the second order approximation Hamiltonian and the original Hamiltonian (see text) respectively.

Notice that  $|\psi(0)\rangle$  belongs to the subspace  $V^{(0)}$ , and the time evolution will be restricted in this subspace. Fig5(a) gives the probabilities  $P_i(t) = |\langle i|\psi(t)\rangle|^2$  of finding state  $|i\rangle$  at time  $t$ , where  $|i\rangle$  stands for the four bases of the subspace  $V^{(0)}$ :  $|\uparrow\downarrow, 0_A, 0_a\rangle$ ,  $|\downarrow\uparrow, 0_A, 0_a\rangle$ ,  $|\downarrow\downarrow, 1_A, 0_a\rangle$ , and  $|\downarrow\downarrow, 0_A, 1_a\rangle$  respectively. Besides the states  $|\uparrow\downarrow, 0_A, 0_a\rangle$  and  $|\downarrow\uparrow, 0_A, 0_a\rangle$ , the unwanted boson modes excitation states  $|\downarrow\downarrow, 1_A, 0_a\rangle$ , and  $|\downarrow\downarrow, 0_A, 1_a\rangle$  also have nonzero populations. This populations will induce the gate error. Furthermore, we calculate the fidelity function defined by

$$F(t) = \left| \langle \psi(0) | U_{\sqrt{i}\text{SWAP}}^+ U(t) | \psi(0) \rangle \right|, \quad (40)$$

where  $U_{\sqrt{i}\text{SWAP}}$  is the ideal  $\sqrt{i}\text{SWAP}$  gate operator. We notice that the fidelity function  $F(t)$  reaches its maximum slightly less than unity at  $t = t_0$ , and the high-frequency oscillations appear due to the boson modes excitation mentioned above. We also examine the fidelity function generated by the original Hamiltonian (31), i.e.  $U(t) = \exp[-it(H_0 + H_1)/\hbar]$ . In this case the original Hamiltonian (31) gives a high fidelity  $F(t') \simeq 1$  at a different time  $t' \simeq 1.2t_0$ , which can be regarded as the higher order correction in comparison to the approximate

Hamiltonian (33). Finally, Fig.5 shows that spin entanglement can be created in this system by adjusting the operation time.

## V. CONCLUSION

In this paper, we have considered a system of two vertically CQDs each containing an electron in the presence of Rashba type SOI. We theoretically demonstrate that it is possible to create spin entanglement in this kind of system by using the SO coupling. With the large inter-dot separation case, the Coulomb interaction between the two electrons is approximately expressed in a quadratic form. And then two-boson-two-spin interacting model is derived in the RWA from the original Hamiltonian. We give the exact solution of the low excitation states analytically. This solution helps us reveal the physics under the FIR spectra near the resonant point. Perturbation treatment in the large detuning case shows that, similar to the quantum dot embedded in an optical cavity, the orbital freedoms play a role of quantized data bus via the

Coulomb interaction and SOI in this system. An effective Hamiltonian of spin-spin interaction is obtained in the perturbation regime by eliminating the orbital freedoms. This Hamiltonian provides a two-qubit operation, which is essential in quantum information processing.

Finally, we would like to point out that using the effective inter-spin coupling to create spin entanglement is feasible to be controlled and measured. From the discussion above, we know that the effective spin coupling strength can be controlled by external magnetic field. On the other hand, the tuneable strength of SOI  $\alpha$  [11], in principle, also enable us to switch on and off the effective inter-spin coupling by external gates conveniently. To probe the quantum entanglement of spin system, similar method in the protocol proposed in ref. [23] can be used, where the information stored in the spin degrees of freedom is converted to the charge states, and then the charge states can be detected.

This work is funded by NSFC with grant Nos. 90203018, 10474104, 60433050, 10374057, 10574077 and NFRPC with Nos. 2001CB309310, 2005CB724508, 2005CB623606.

- 
- [1] I. Zutic, Rev. Mod. Phys. **76**(2), 323 (2004)
  - [2] D. D. Awschalom *et. al.*, Semiconductor Spintronics and Quantum Computation, (Springer-Verlag, Berlin, 2002)
  - [3] S. Debal, Phys. Rev. Lett. **94**, 226803 (2005)
  - [4] M. Governale, Phys. Rev. Lett. **89**, 206802 (2002)
  - [5] P. Lucignano *et. al.*, Phys. Rev. B **71**, 121310(R) (2005)
  - [6] T. Chakraborty, Phys. Rev. Lett. **95**, 136603 (2005)
  - [7] P. Pietilainen and T. Chakraborty, cond-mat/0509170
  - [8] T. Chakraborty and P. Pietilainen, Phys. Rev. B **71**, 113305 (2005)
  - [9] P. Stano *et. al.*, Phys. Rev. B **72**, 155410 (2005)
  - [10] P. Splettstoesser, Phys. Rev. B **68**, 165341 (2003)
  - [11] S. Debal, Phys. Rev. B **71**, 115322 (2005)
  - [12] M. Bayer *et. al.*, Science **291**, 451 (2001); Jia-Lin Zhu *et. al.*, Phys. Rev. B **72**, 165346 (2005); Xiaoqin Li *et. al.*, Science **301**, 809 (2003)
  - [13] W. Yao, R. Liu, and L. J. Sham, Phys. Rev. Lett. **92**, 217402 (2004); **95**, 030504 (2005); R.-B. Liu, W. Yao, and L. J. Sham; Phys. Rev. B **72**, 081306 (2005);
  - [14] Y. Li, T. Shi, B. Chen, Z. Song, and C.-P. Sun, Phys. Rev. A **71**, 022301 (2005); T. Shi, Y. Li, Z. Song, and C.-P. Sun; Phys. Rev. A **71**, 032309 (2005); Z. Song, P. Zhang, T. Shi, and C.-P. Sun; Phys. Rev. B **71**, 205314 (2005).
  - [15] A. Imamoglu, Phys. Rev. Lett. **83**, 4204 (1999)
  - [16] O. Gywat *et. al.*, cond-mat/0511592; G. Burkard and Atac Imamoglu, cond-mat/0603119
  - [17] N. F. Johnson and M. C. Payne, Phys. Rev. Lett. **67**, 1157 (1990)
  - [18] B. L. Johnson and G. Kirczenow, Phys. Rev. B **47**, 10563 (1993)
  - [19] L. Wendler *et. al.*, Phys. Rev. B **54**, 4794 (1996)
  - [20] H. Hu *et. al.*, Phys. Rev. B **62**, 16777 (2000)
  - [21] Lucjan Jacak *et. al.*, Quantum Dots, (Springer-Verlag, Berlin, 1998)
  - [22] A. Blais *et. al.*, Phys. Rev. A **69**, 062320 (2004)
  - [23] H-A. Engel and D. Loss, Science **309**, 586 (2005)